

## Temperature Dependence of the Luminescence Lifetime of Single CdSe/ZnS Quantum Dots

Olivier Labeau, Philippe Tamarat, and Brahim Lounis

*Centre de Physique Moléculaire Optique et Hertzienne, CNRS et Université Bordeaux I,  
351 Cours de la Libération, 33405 Talence Cedex, France*

(Received 19 November 2002; published 26 June 2003)

We study the temperature dependence of the luminescence decay of single CdSe/ZnS quantum dots between 2 and 140 K. For the first time, we observe a biexponential decay which was completely hidden in ensemble measurements. We find that the long time component strongly depends on temperature. This demonstrates that the band edge luminescence arises from two thermally mixed fine structure states, the dark ground state and the lowest bright one. To interpret our results, we derive the analytical expressions for the decay using a three level model. Fitting the experimental data leads directly to the lifetime of the states as well as their energy splitting.

DOI: 10.1103/PhysRevLett.90.257404

PACS numbers: 78.67.Hc, 78.55.Et

Over the past decade, interest in low-dimensional, mesoscopic systems, such as quantum dots (QDs), has grown dramatically. These semiconductor QDs bridge the gap between single molecules and the bulk solid state, thereby offering the opportunity to study the evolution of bulk properties. Additionally, their size-dependent optical properties make them ideal candidates for tunable absorbers and emitters in applications such as nanoscale electronics [1–3], laser technology [4], and biological fluorescent labeling [5,6]. Chemically synthesized CdSe QDs are promising for many of these applications due to their bright luminescence, which is size tunable across the visible spectrum [7,8].

The electronic properties of nanocrystals with dimensions smaller than the bulk exciton Bohr radius are dominated by quantum confinement effects. The band edge exciton ( $1S_{3/2}1S_e$ ), which is eightfold degenerate in spherically symmetric dots [9,10], is split into five levels by the crystal shape asymmetry, the intrinsic crystal field, and the enhanced electron-hole exchange interaction. The exciton ground state is located a few meV below the lowest-energy optically active ( $J = \pm 1^L$ ) exciton state, and has a total spin projection on the crystal hexagonal axis  $J = \pm 2$ . While optical transitions to and from this state are normally forbidden within the electric dipole approximation, radiative recombination from this state can occur with the emission or absorption of phonons. At low temperatures, these processes are much slower than those of direct optical recombination. This leads to the formation of a long-lived exciton state.

Low temperature fluorescence line narrowing and photoluminescence spectra, measured on ensembles of CdSe QDs, support the picture of dark exciton formation via excitation of higher energy fine structure states followed by rapid thermalization to the exciton ground state [9]. The photoluminescence comes primarily from the recombination of the dark state. It is redshifted with respect to a resonant excitation frequency and has long radiative lifetimes ( $\sim 1 \mu\text{s}$  at 10 K) relative to the bulk exciton recombination time ( $\sim 1 \text{ ns}$ ). Mixing of the bright and dark

excitons in an external magnetic field allows a direct optical recombination of the dark exciton and shortens the luminescence decay time of CdSe QDs [10,11]. The radiative pathway of this nominally forbidden transition is not fully understood.

Time correlated single photon counting (TCSPC) technique performed on ensembles of QDs always led to multiexponential luminescence decays [9–12] because of the sample inhomogeneities (e.g., in size, surface, and shape). This prevented any quantitative temperature dependence investigation and hid any multiple decay behavior of the system. Since its inception, single nano-objects methods have improved our understanding of fluorescent systems by elucidating the photophysics of isolated species in the absence of ensemble averaging [13]. The study of QDs has already benefited from these methods, including the discovery of spontaneous spectral shifts [14], ultranarrow transitions [15], and fluorescence intermittence [16].

At room temperature, lifetimes of the excitonic ground manifold were first deduced from the luminescence intensity correlation function of single CdSe QDs in photon antibunching measurements [17]. The lifetimes ranged between 12 and 28 ns with a mean value around 18 ns. Recently, TCSPC experiments performed on single QDs showed a multiexponential luminescence decay which was attributed to changes of the single QD lifetime during the accumulation time [18]. Correlation between the blinking effect and a fluctuating dynamic process was hypothesized.

In this Letter, we study for the first time the temperature dependence of single QD luminescence lifetimes in the range 2–140 K. This dependence provides a new insight into the exciton recombination mechanisms.

Samples of ZnS-coated CdSe QDs (1.9 nm radius, 565 nm peak emission) are prepared by spin coating clean glass coverslips with a  $10^{-9}$  M solution of QDs in toluene, followed by 2% by weight poly(methyl methacrylate)/toluene solution. The excitation beam is the 514 nm line of a mode-locked Ar<sup>+</sup> laser (120 ps pulse width). The

repetition rate of the laser beam is reduced with a pulse picker in order to study the long decays. Single QDs are imaged with a homebuilt laser scanning confocal microscope. It is based on a pair of galvano-driven mirrors, a telecentric lens system, and a 0.95 NA objective which is inserted in a helium cryostat together with the sample. The emitted photons are filtered from the scattered excitation light by a bandpass filter (70 nm full width at half maximum) and sent to a single-photon-counting avalanche photodiode. The luminescence decay is measured using classical TCSPC with a time resolution limited to few hundreds of picoseconds.

Figure 1(a) presents the luminescence decay of a bulk solution of QDs recorded at 16 K. Because of the inhomogeneous distribution of QD lifetimes, it shows a multi-exponential behavior distributed on a large time scale. In Fig. 1(b), we present a typical decay curve of a single QD recorded at the same temperature. It clearly shows a biexponential behavior which is completely hidden in the ensemble measurement of Fig. 1(a). It has a very fast decay occurring within our time resolution scale (a few hundreds of ps) and a much slower one with a lifetime  $\tau_L$  in the 100 ns range. The time integrated signal corresponding to the fast component amounts to less than 1% of the total signal. Most of the studied QDs (more than 80 over 100) showed a similar biexponential behavior. At higher temperatures, 140 K for Fig. 1(c),  $\tau_L$  shortens considerably and the fast component vanishes completely.

Measurements of  $\tau_L$  were then carried out at different temperatures on a large number of single QDs. Each

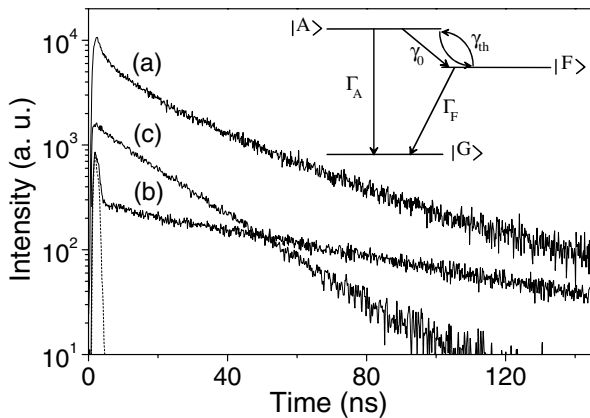


FIG. 1. Typical luminescence decay curves of CdSe/ZnS QDs. (a) An ensemble measurement (at 16 K) gives a multi-exponential decay. (b) A single QD decay is biexponential at 16 K. The short time is within our time resolution and the long decay time is around 73 ns. (c) A single QD decay is mono-exponential at 140 K with a typical lifetime of 19 ns. Inset: The three-state model.  $|G\rangle$  is the zero exciton ground state. The “bright” state  $|A\rangle$  and the “dark” state  $|F\rangle$  are the two lowest states of the band edge exciton with respective lifetimes  $\Gamma_A^{-1}$  ( $\sim 10$  ns) and  $\Gamma_F^{-1}$  ( $\sim 1$   $\mu$ s).  $\gamma_0 \sim 10$  ns $^{-1}$  is the zero temperature  $|A\rangle \rightarrow |F\rangle$  relaxation rate.  $\gamma_{th}$  is the thermalization rate due to the interaction with an acoustic phonon mode.

histogram of Fig. 2 is built from approximately 100 single QDs. One can clearly see [Fig. 3(a)] that the average decay rate increases with temperature and saturates at temperatures higher than 70 K. The average count rate (under continuous wave excitation) detected from single QDs decreases dramatically below this temperature (more than a factor of 10 between 140 and 5 K). These observations suggest that the emission occurs from two thermally populated states, a weakly emitting long-lived ground state, and a strongly emitting upper one.

The temperature dependence of the decay curves is modeled on the basis of a three level system (see Fig. 1): a zero exciton ground level  $|G\rangle$ , and two excitonic states  $|F\rangle$  and  $|A\rangle$  representing, respectively, the dark ( $J = \pm 2$ ) and the bright ( $J = \pm 1^L$ ) excitons, with recombination rates  $\Gamma_F$  and  $\Gamma_A$ . The energy splitting  $E_{AF}$  between these two states is in the few meV range, depending on the size and shape of the QDs [9,10]. Emission and absorption of acoustic phonons from a mode whose energy  $\Delta E$  matches  $E_{AF}$  induces a thermalization of the excitonic states. The  $|A\rangle \rightarrow |F\rangle$  and  $|F\rangle \rightarrow |A\rangle$  rates are, respectively,  $\gamma_0(N_B + 1)$  and  $\gamma_0 N_B = \gamma_{th}$ , where  $N_B = 1/[\exp(\Delta E/k_B T) - 1]$  is

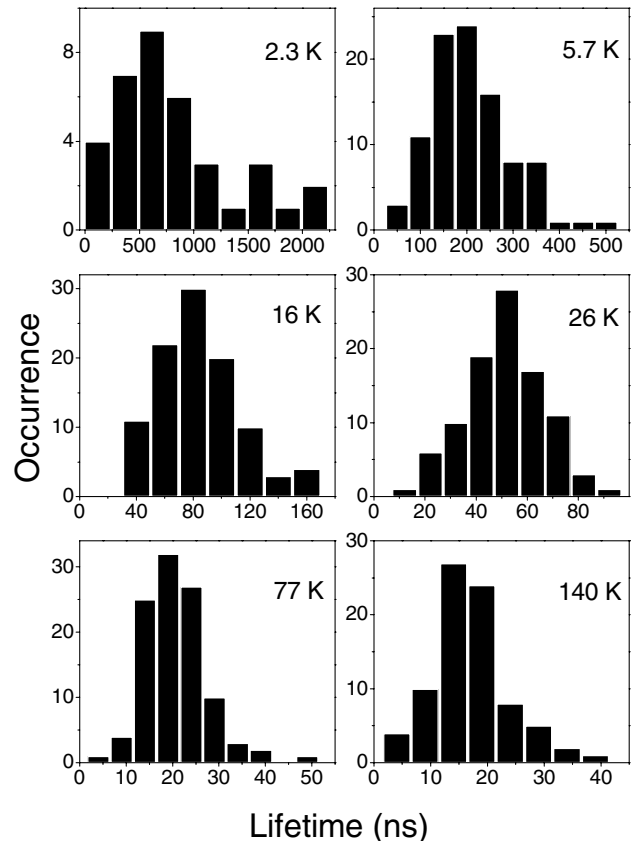


FIG. 2. Histograms of the long component decay time  $\tau_L$  built from about a hundred single QDs at various temperatures (between 2.3 and 140 K). The mean  $\tau_L$  values are 865 ns at 2.3 K, 209 ns at 5.7 K, 85 ns at 16 K, 51 ns at 77 K, and 19 ns at 140 K.

the Bose-Einstein phonon number at the temperature  $T$ .  $\gamma_0$  is the zero temperature relaxation rate of the  $|A\rangle \rightarrow |F\rangle$  transition.

We use rate equations to derive the time evolution of the two populations  $p_F$  and  $p_A$  of the excitonic states, after a short pulsed laser excitation at  $t = 0$  which leads to initial populations  $p_A(0)$  and  $p_F(0)$  [with  $p_F(0) + p_A(0) = 1$ ]. The luminescence signal  $S(t)$  is proportional to  $(\eta_A \Gamma_A p_A + \eta_F \Gamma_F p_F)$ , where  $\eta_A$  and  $\eta_F$  are the radiative yields of states  $|A\rangle$  and  $|F\rangle$ , respectively. Considering the approximation  $\gamma_0 \gg \Gamma_A \gg \Gamma_F$ , we find

$$S(t) = \frac{\eta_A \Gamma_A N_B + \eta_F \Gamma_F}{1 + 2N_B} \exp\left(-\frac{t}{\tau_L}\right) + \eta_A \Gamma_A \left[ p_A(0) - \frac{N_B}{1 + 2N_B} \right] \exp\left(-\frac{t}{\tau_S}\right), \quad (1)$$

where  $\tau_S$  and  $\tau_L$  are, respectively, a short and a long characteristic time given by

$$\tau_S^{-1} = \gamma_0(1 + 2N_B) \quad \text{and} \\ \tau_L^{-1} = \frac{\Gamma_A + \Gamma_F}{2} - \left( \frac{\Gamma_A - \Gamma_F}{2} \right) \tanh\left\{ \frac{\Delta E}{2k_B T} \right\}. \quad (2)$$

In the high temperature regime, where  $k_B T \gg \Delta E$  ( $N_B \gg 1$ ), the amplitude of the fast component vanishes for  $p_A(0) = p_F(0) = 1/2$ . This means that the two lowest excitonic levels are equally populated from the high energy continuum states which are initially prepared by the laser pulse [19]. In this case, the signal shows a single exponential decay and writes  $S_{T>}(t) = (\eta_A \Gamma_A / 2) \times \exp(-\Gamma_A t / 2)$ . The luminescence stems from the bright exciton state and exhibits a decay time which is twice the lifetime of the state  $|A\rangle$ . However, in the low temperature regime ( $k_B T \ll \Delta E$  and  $N_B \ll 1$ ), the signal shows a biexponential decay and is given by  $S_{T<}(t) = \eta_F \Gamma_F \times \exp(-\Gamma_F t) + (\eta_A \Gamma_A / 2) \exp(-\gamma_0 t)$ . The ratio between the time integrated signals of the fast and slow components is then  $\eta_A \Gamma_A / 2 \eta_F \gamma_0$ . For typical values  $\Gamma_A \sim 0.1 \text{ ns}^{-1}$ ,  $\eta_A \sim \eta_F \sim 1$ , and  $\gamma_0 > 1 \text{ ns}^{-1}$  [9,20], this ratio is less than a few percent, in agreement with our experimental observations.

The stability of our experimental setup allows us to follow the behavior of a single QD on a large temperature range. The inset of Fig. 3(b) shows the long time component of the luminescence decay recorded on the same QD at different temperatures (between 2.7 and 28 K). The shortening of the lifetime with temperature is well reproduced by the expression (2) [see middle curve of Fig. 3(b)]. The fit leads to  $\Gamma_A$ ,  $\Gamma_F$ , and  $\Delta E$ , the three relevant parameters involved in the QD luminescence. The energy  $\Delta E$  of the acoustic phonon mode responsible for the thermalization matches the energy splitting  $E_{AF}$  between the lowest exciton states. We performed this measurement on 15 single QDs and found  $1.3 \text{ meV} < E_{AF} < 3.8 \text{ meV}$ .

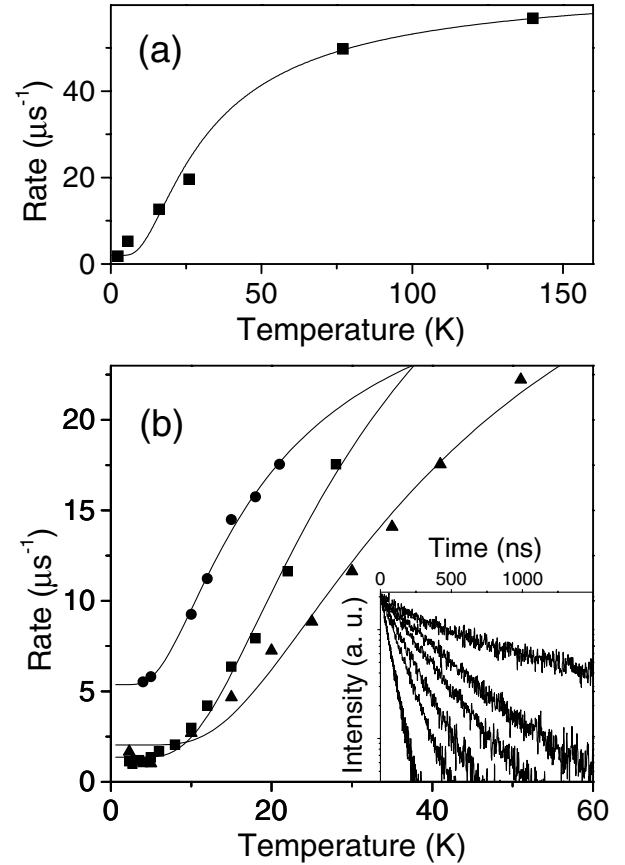


FIG. 3. (a) Evolution with temperature of the mean decay rate  $\tau_L^{-1}$  deduced from the histograms of Fig. 2. The continuous curve is theoretical rates of Eq. (2), plotted with  $\Gamma_A = 0.13 \text{ ns}^{-1}$ ,  $\Gamma_F = 2 \mu\text{s}^{-1}$ , and  $\Delta E = 3.5 \text{ meV}$ . (b) Inset: luminescence decay curves of a single QD, recorded at temperatures 2.7, 10, 12, 15, 18, and 28 K. For clarity, the first 10 ns of the curves are not presented and the data are normalized. (b) Main figure: Temperature dependence of the long component rate, for three single QDs with different radius (circles for the “red” QD, radius 5.6 nm; squares for the “yellow” QD, radius 1.9 nm; triangles for the “green” QD, radius 1.5 nm). The experimental points are well fitted with the expression of  $\tau_L^{-1}$  deduced from the thermal mixing model. The fits give  $\Gamma_F = 5.4 \mu\text{s}^{-1}$ ,  $\Gamma_A = 57 \mu\text{s}^{-1}$ ,  $E_{AF} = 2.1 \text{ meV}$  for the “red” QD;  $\Gamma_F = 1.4 \mu\text{s}^{-1}$ ,  $\Gamma_A = 92 \mu\text{s}^{-1}$ ,  $E_{AF} = 3.8 \text{ meV}$  for the “yellow” QD;  $\Gamma_F = 2.0 \mu\text{s}^{-1}$ ,  $\Gamma_A = 82 \mu\text{s}^{-1}$ ,  $E_{AF} = 5.0 \text{ meV}$  for the “green” QD.

The expression (2) of the long component decay rate  $\tau_L^{-1}$  reproduces satisfactorily the temperature dependence of the average rates calculated from the histograms [see Fig. 3(a)]. The solid curve is plotted for average values of the rates  $\Gamma_A = 0.13 \text{ ns}^{-1}$  and  $\Gamma_F = 2 \mu\text{s}^{-1}$  and an energy splitting  $\Delta E = 3.5 \text{ meV}$  (typical for 1.9 nm QD radius).

When we study smaller size QDs (1.5 nm radius, peak emission 538 nm), we find the same overall luminescence decay behavior. The decay rates are comparable to those of the previous QDs. As expected, we obtain higher activation temperatures [see right curve of Fig. 3(b)] corresponding to larger splitting energies

( $3.6 \text{ meV} < E_{AF} < 7 \text{ meV}$  for six QDs). This is due to the enhancement of the electron-hole exchange interaction when the QD size decreases [9]. The large dispersion in the splitting energies is attributed to the size and shape distribution of the QDs. However, most of the measurements performed on QDs with a larger size (5.6 nm radius, peak emission 640 nm) show a multiexponential luminescence decay on a large time scale at low temperatures. For these large QDs, the size is comparable to the bulk exciton Bohr radius. Therefore, the strong confinement regime is not reached and the presented model is no longer valid. Some QDs ( $\sim 20\%$ ) show a short time multiexponential decay, followed by a long time monoexponential one. The left curve of Fig. 3(b) displays a typical evolution of  $\tau_L^{-1}$  with temperature for such QDs. The fit gives a splitting energy of  $\sim 2 \text{ meV}$ . These QDs may be small-radius particles of the size distribution edge, or may present deviant shapes.

In summary, we studied for the first time the temperature behavior of the luminescence decay of single QDs. We showed that the luminescence arises from the two thermally mixed lowest states of the band edge exciton fine structure. Contrary to room temperature measurements [17,18] which only lead to an effective lifetime resulting from the thermalization of all the fine structure levels of the exciton state, the temperature dependence of the luminescence decay gives access to the bright and the dark exciton lifetimes, as well as their energy splitting. In contradiction with what was reported for self-assembled CdSe/ZnSe QDs [21], our results show that the bright exciton radiative decay rate  $\Gamma_A$  is much smaller than the spin flip  $|A\rangle \rightarrow |F\rangle$  rate  $\gamma_0$ .

For the dark state, a dipole radiative transition is forbidden and the emission can occur through interaction with phonons. A long lifetime  $\Gamma_F^{-1}$  of the dark state is consistent with a longitudinal optical (LO) phonon assisted recombination [19,20]. However, the zero LO phonon line observed in the photoluminescence suggests an alternate recombination pathway through coupling to acoustic phonons [22]. Other recombination mechanisms may involve spin flip transitions induced by paramagnetic defects in the lattice or a high order interaction with

phonons. Surface states may also have a strong influence on the relaxation mechanisms of this weakly emitting dark state. This would explain the large relative distribution of  $\tau_L$  observed at very low temperatures.

Further experiments will be the investigation of the effect of an applied magnetic field on the luminescence decay, as well as the measurement of the optical coherence lifetime of the dark exciton state.

We thank Michel Orrit for helpful discussions. This research was funded by CNRS (Individual Nano-Object Program), Région Aquitaine, and the French Ministry for Education and Research (MENRT).

- 
- [1] M. Schlamp, X. Peng, and A. P. Alivisatos, *J. Appl. Phys.* **82**, 5837 (1997).
  - [2] B. O. Dabbousi *et al.*, *Appl. Phys. Lett.* **66**, 1316 (1995).
  - [3] V. L. Colvin, M. C. Schlamp, and A. P. Alivisatos, *Nature (London)* **370**, 354 (1994).
  - [4] V. I. Klimov *et al.*, *Science* **290**, 314 (2000).
  - [5] M. Bruchez, Jr. *et al.*, *Science* **281**, 2013 (1998).
  - [6] B. Chan *et al.*, *Proc. Natl. Acad. Sci. U.S.A.* **96**, 459 (1999).
  - [7] A. P. Alivisatos, *Science* **271**, 933 (1996).
  - [8] D. J. Norris *et al.*, *Phys. Rev. Lett.* **72**, 2612 (1994).
  - [9] A. L. Efros *et al.*, *Phys. Rev. B* **54**, 4843 (1996).
  - [10] M. Nirmal *et al.*, *Phys. Rev. Lett.* **75**, 3728 (1995).
  - [11] E. Johnston-Halperin *et al.*, *Phys. Rev. B* **63**, 205309 (2001).
  - [12] M. G. Bawendi *et al.*, *J. Chem. Phys.* **96**, 946 (1992).
  - [13] W. E. Moerner and M. Orrit, *Science* **283**, 1670 (1999).
  - [14] S. A. Empedocles and M. G. Bawendi, *Science* **278**, 2114 (1997).
  - [15] S. A. Empedocles, D. J. Norris, and M. G. Bawendi, *Phys. Rev. Lett.* **77**, 3873 (1996).
  - [16] M. Nirmal *et al.*, *Nature (London)* **383**, 802 (1996).
  - [17] B. Lounis *et al.*, *Chem. Phys. Lett.* **329**, 399 (2000).
  - [18] G. Schlegel *et al.*, *Phys. Rev. Lett.* **88**, 137401 (2002).
  - [19] A. L. Efros, *Phys. Rev. B* **46**, 7448 (1992).
  - [20] M. Chamorro *et al.*, *Phys. Rev. B* **53**, 1336 (1996).
  - [21] G. Bacher *et al.*, *Phys. Rev. Lett.* **83**, 4417 (1999).
  - [22] U. Woggon *et al.*, *Phys. Rev. B* **54**, 1506 (1996).